

# Characterization of Mismatches in Time-Interleaved ADC

Manel Ben-Romdhane<sup>1</sup>, Asma Maalej<sup>1</sup>, Chiheb Rebai<sup>1</sup> and Dominique Dallet<sup>2</sup>

<sup>1</sup> GRESCOM Research Lab., SUP'COM, University of Carthage, Tunisia  
[manel.benromdhane@supcom.rnu.tn](mailto:manel.benromdhane@supcom.rnu.tn),  
[asma.maalej@supcom.rnu.tn](mailto:asma.maalej@supcom.rnu.tn),  
[chiheb.rebai@supcom.rnu.tn](mailto:chiheb.rebai@supcom.rnu.tn)

<sup>2</sup> IMS Research Lab., IPB ENSEIRB-MATMECA, University of Bordeaux, France  
[dominique.dallet@ims-bordeaux.fr](mailto:dominique.dallet@ims-bordeaux.fr)

**Abstract**—Time-interleaved analog to digital converter (TI-ADC) is a technique of increasing sampling frequencies and bandwidth while keeping high resolution. In this paper, the authors aim to characterize a TI-ADC with mismatches. They propose equivalent scheme and identification to time-quantized pseudorandom sampling technique. The goal of this identification is to enable the adaptation of mismatch compensation technique of TI-ADC to recover mismatches in ADC acquisition using time-quantized pseudorandom sampling.

## I. INTRODUCTION

As the wideband applications grow, the software defined radio receivers need faster analog-to-digital converters (ADC) with higher resolutions and larger analog bandwidth [1]. This has to come also with power efficient circuits or architectures. The ADC researchers' community focuses on the solution of parallel ADC. In fact, Instead of design a single very high speed and high resolution ADC, it was proposed to use a parallel architecture of multiple slower and high resolution ADCs as the time-interleaved ADC (TI-ADC) [2], the frequency band decomposition (FBD) parallel ADC [3] and Hadamard modulated parallel ADC [4]. However, implementing such parallel ADC is not trivial and requires corrections of parallel ADC mismatches [5-7].

In this paper, the authors focus on the TI-ADC because of its simple concept of using the same ADC  $M$  times but also for its similarity to non-uniform sampling in presence of mismatches. As mentioned in [6, 8], TI-ADC with imperfections causes a periodical non-uniform sampling. However, to our best knowledge, there is no previous work on the characterization of the mismatches in TI-ADC by time-quantized pseudorandom sampling (TQ-PRS) technique. Further, the proposed work is the basis that will allow authors to use compensation technique of TI-ADC mismatches to recover mismatches in ADC acquisition using time-quantized pseudorandom sampling.

This paper is organized as follows. Section II reviews the TI-ADC operation pointing out offset, gain and clock skew mismatches effects on the sampled signal. Section III presents the proposed equivalent scheme of the TI-ADC technique with different mismatches and proposes identification with TQ-PRS technique. Section IV presents a comparison between simulation results of the two previously techniques and test results. Finally, conclusions are drawn in Section V.

## II. TI-ADC MODELING

### A. Principle of TI-ADC

TI-ADC objective is to reach high output resolution at high sampling frequency [2]. An ideal TI-ADC is illustrated by Fig. 1. Indeed, the input signal is sampled by  $M$  identical  $ADC_l$ ,  $0 \leq l \leq M - 1$ , at a similar sampling frequency,  $f_s/M$ , but using  $M$  different clock phases,  $\phi_0, \phi_1, \dots, \phi_{M-1}$ , as described in Fig. 2. Thus, the  $l^{th}$  sampling instant is equal to  $kMT_s + lT_s$ . All the ADC outputs are processed by a digital multiplexer at a sampling frequency,  $f_s = 1/T_s$ , to obtain,  $y(k)$ . The described technique conserves the single ADC resolution and increases  $M$  times the single ADC sampling frequency and therefore the effective analog bandwidth.

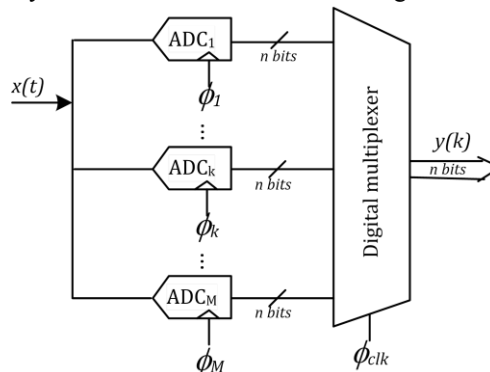


Fig. 1. Scheme of an ideal  $M$ -branch TI-ADC.

### B. TI-ADC sampling effect

The TI-ADC process is composed of sampling and quantization operations. In this paper, the authors focus only on sampling process, thus, the TI-ADC converts a continuous analog bandpass signal,  $x(t)$ , into its discrete  $y(t)$  representation, as given by (1) [6].

$$y(t) = \sum_{l=0}^{M-1} x(t) \sum_{k=-\infty}^{+\infty} \delta(t - kMT_s - lT_s) \quad (1)$$

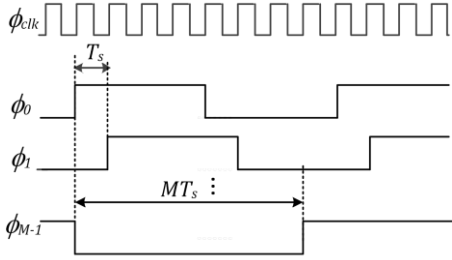


Fig. 2. Timing for a TI-ADC.

The Fourier transform of  $y(t)$  is obtained as in (2) where the coefficient  $C_k$  is written as in (3).

$$Y(f) = \frac{1}{T_s} \sum_{k=-\infty}^{+\infty} C_k X\left(f - \frac{kf_s}{M}\right) \quad (2)$$

$$C_k = \frac{1}{M} \sum_{l=0}^{M-1} e^{-j2\pi kl/M} \quad (3)$$

The expression  $C_k$  is a geometric sequence with a common factor  $e^{-j2\pi l/M}$  and a first factor  $1/M$ . Therefore,  $C_k$  becomes as in (4).

$$C_k = e^{-j\pi k(1-\frac{1}{M})} \frac{\text{sinc}(\pi k)}{\text{sinc}\left(\frac{\pi k}{M}\right)} = \begin{cases} 1 & \text{if } k = nM, n \in \mathbb{Z} \\ 0 & \text{unless} \end{cases} \quad (4)$$

The coefficients  $C_k$  cancel the replicas terms  $X\left(f - \frac{kf_s}{M}\right)$  for  $k \neq nM$  which are obtained from the sampling operation at  $f_s/M$  of each ADC. Hence,  $Y(f)$ , as written in (5), contains only the replicas of the input signal as if it were sampled at  $f_s$ .

$$Y(f) = \frac{1}{T_s} \sum_{k=-\infty}^{+\infty} X(f - kf_s) \quad (5)$$

### C. Mismatches in TI-ADC

The above single ADCs, particularly the sampling operations, are assumed to be identical. However, due to the current analog CMOS fabrication process, there are mismatches which are assumed to be constant over time for a given ADC. The three main mismatches are offset

mismatch, gain mismatch and clock skew mismatch [6]. The  $ADC_l$  offset mismatch,  $o_l$ , is modeled by an added constant to the input signal. The  $ADC_l$  gain mismatch,  $g_l$ , is modeled by a multiplicative factor on the input signal. The  $ADC_l$  clock skew mismatch,  $\tau_l$ , is a constant delay between the ideal and real sampling instants. The scheme of an M branch TI-ADC with mismatches is presented in Fig. 3 [6].

The TI-ADC with mismatches converts a continuous analog bandpass signal,  $x(t)$ , into its discrete  $\tilde{y}(t)$  representation, as given by (6).

$$\tilde{y}(t) = \sum_{k=-\infty}^{+\infty} \sum_{l=0}^{M-1} ((1 + g_l)x(t + \tau_l) + o_l) \cdot \delta(t - kMT_s - lT_s) \quad (6)$$

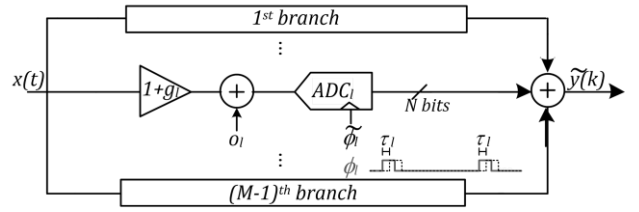


Fig. 3. Scheme of an M-branch TI-ADC with offset, gain and clock skew mismatches.

The computation result of Fourier transform is then obtained as in (7)

$$\tilde{Y}(f) = \frac{1}{T_s} \sum_{k=-\infty}^{+\infty} \left[ (G_k + S_k) X\left(f - \frac{kf_s}{M}\right) + O_k \delta\left(f - \frac{kf_s}{M}\right) \right] \quad (7)$$

where the coefficients  $G_k$ ,  $S_k$  and  $O_k$  are written as in (8).

$$G_k = \frac{1}{M} \sum_{l=0}^{M-1} g_l e^{-\frac{j2\pi kl}{M}}$$

$$S_k = \frac{1}{M} \sum_{l=0}^{M-1} e^{-j2\pi f(lT_s + \tau_l)} \quad (8)$$

$$O_k = \frac{1}{M} \sum_{l=0}^{M-1} o_l e^{-\frac{j2\pi kl}{M}}$$

From (7), the offset mismatch introduces spurious replicas at  $kf_s/M$ . These replicas are independent of the signal and are dependent only of the values of the sampling frequency, the number of branches of the TI-ADC and the offset errors. However, both of gain and clock skew mismatches causes replicas of the input signal spectrum to appear centered around integer multiples of branch sampling frequency,  $f_s/M$ . Only the power levels of the replicas due to clock skew mismatch are dependent of the signal frequency. From (7), the authors propose an equivalent model of the TI-ADC with mismatches.

### III. PROPOSED EQUIVALENT MODEL OF THE TI-ADC

#### A. Proposed equivalent model

As presented by equation (7), the M TI-ADC branches can be replaced by an ADC which is driven by a specific signal relative to the clock skew. The gain in the equivalent model is an array including gains in the M branches. The offset value is also selected within M values corresponding to the selected branch in TI-ADC. The equivalent model is given by Fig. 4.

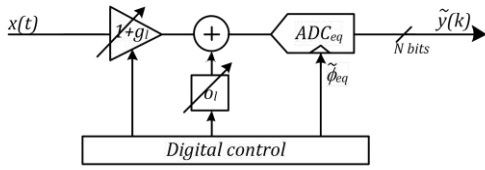


Fig. 4. Equivalent scheme of the TI-ADC with offset, gain and clock skew mismatches.

The selection of the corresponding gain and offset is achieved by a digital control block. Besides, this block provides an equivalent phase  $\tilde{\phi}_{eq}$  that copies pseudorandomly the period  $\tilde{\phi}_l$  of the  $l$ th branch in TI-ADC including its clock skew. Therefore, the digital control includes a distortion generator that substitutes the phases commanding the TI-ADC branches  $\tilde{\phi}_0, \dots, \tilde{\phi}_{M-1}$  by the equivalent signal  $\tilde{\phi}_{eq}$  shown in Fig. 5.

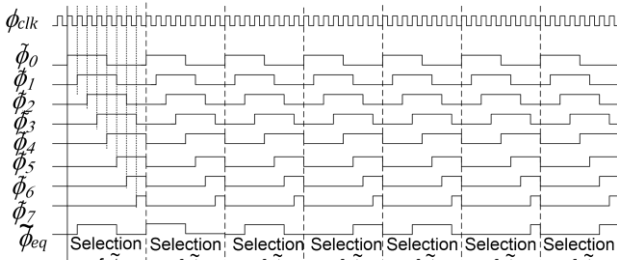


Fig. 5. Equivalent clock of 8-branch TI-ADC considering clock skew mismatches.

#### B. Identification with pseudorandomly sampled signals

Each kind of mismatch has a different impact on the signal spectrum as detailed in section II. For offset and gain mismatches, the output signal power is constant as the input frequency applied to the ADC increases. Besides, for the clock skew mismatch, the signal power decreases when as the input frequency increases [9]. In this paper, the authors focus only in clock skew mismatch to make the relation between this TI-ADC mismatch and the pseudo-random sampling technique. In fact, having a different clock skew for each branch in TI-ADC leads to

pseudorandom clock skews that appear in  $\tilde{\phi}_{eq}$ . This pseudorandom sequence of clock skews added to pseudorandom selection of ADC generates a pseudorandom instant leading to time-quantized pseudorandom sampling (TQ-PRS) [10]. The equation of such sampling technique has been presented in detail in previous work while specifying different sampling and time quantization parameters [11]. In this work, the authors propose the TQ-PRS formula,  $Y_{TQ-PRS}(f)$ , of an analog signal  $x(t)$  as given by (9).

$$Y_{TQ-PRS}(f) = \frac{f_{PRS}}{q} \sum_{l=0}^{q-1} \sum_{k=-\infty}^{+\infty} e^{-j2\pi f(\alpha_l + lT_{PRS})} X\left(f - k\frac{f_{PRS}}{q}\right) \quad (9)$$

where  $f_{PRS}$  is the mean sampling frequency of the TQ-PRS,  $q$  is the quantization factor of the mean sampling period  $T_{PRS} = 1/f_{PRS}$  and  $\alpha_l$  is the time delay between the  $l$ th sampling instant and its corresponding uniform sampling instant. In case of clock skew mismatch,  $\alpha_l$  is given in (10) where  $T_{PRS}/q$  is the step of time-quantized pseudorandom sampling.

$$\alpha_l = l\frac{T_{PRS}}{q} + \tau_l \quad (10)$$

Analogically to  $S_k$  in (8), the TI-ADC with clock skew mismatch is equivalent to TQ-PRS with a quantization factor  $q$  equal to the TI-ADC number of branches,  $M$ . The mean pseudorandom sampling frequency  $f_{PRS}$  is equal to the TI-ADC sampling frequency,  $f_s$ .

### IV. SIMULATIONS AND TEST RESULTS

The core of the MATLAB simulations is the sampling technique and the core of the test setup is the ADC. The tested input signal is a sine-wave signal to characterize the clock skew mismatch in TI-ADC by the pseudorandomly controlled ADC.

#### A. Simulation results

In this subsection, the authors compare simulation results of the TI-ADC and the TQ-PRS based ADC. Fig. 6 illustrates the digital output spectrum for an 8-branch TI-ADC with clock skew mismatch for a sine-wave signal at a frequency,  $f$ , equal to 250 kHz and an output sampling frequency,  $f_s$ , equal to 15.625 MHz. To clearly observe the effects of the clock skew mismatch, eight deliberately  $\tau_l$  values are chosen. The same values of  $\tau_l$  are added to a pseudorandom signal sampler for  $q$  equal to 8 as illustrated in Fig. 4. For a mean sampling frequency,  $f_{PRS}$ , equal to 15.625 MHz, the time-quantized pseudorandom sampled signal verifies the frequencies of the spurious replicas. However, their power levels are different. In fact, sampling with M ADC is different from pseudorandomly sampling with the same ADC. Besides, the TQ-PRS offers the advantage to attenuate the replica

at the mean sampling frequency [10]. This advantage is not focused in this paper but more results are discussed in [12].

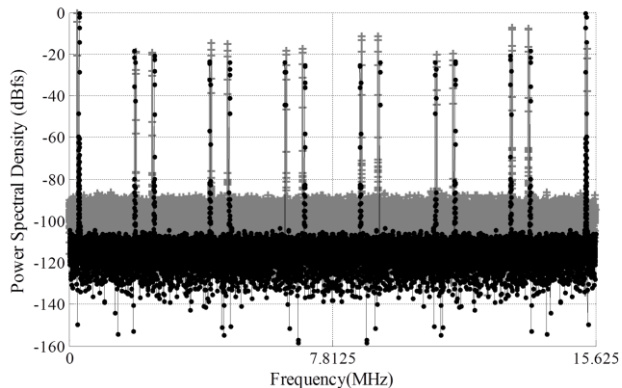


Fig. 6. Spectrum over  $[0, f_s]$  of 8-branches TI-ADC output with clock skew mismatch (black curve) versus TQ-PRS (grey curve).

### B. Distortion generator

A distortion generator is needed to provide the equivalent clock  $\tilde{\phi}_{eq}$  as explained in section III. The authors propose in previous work a distortion generator, the pseudorandom signal sampler (PSS) [13]. The PSS is a digital oscillator that uses a linear feedback shift register (LFSR) to generate a signal with pseudorandom phases. In fact, the LFSR selects one of the signals  $\tilde{\phi}_0, \dots, \tilde{\phi}_{M-1}$ . This selection is equivalent to multiplexer selection of branch  $l$  in TI-ADC.

Another way to generate distortion is proposed via the pseudorandom direct sampler (PDS) [14]. The basic concept of PDS inherits from the direct digital synthesizer, DDS. A pseudorandom sequence given by an LFSR commands a phase increment LUT that stores a phase increment word value  $\Delta P$ . At each clock pulse,  $\Delta P$  is added to a register containing the phase value. This value indexes a sine wave value in a ROM memory in order to give the equivalent sine wave bit sign.

### C. Test results

The acquisition is operated for the same conditions as MATLAB simulation. The PSS (or PDS) and acquisition main clock is a 125 MHz square wave. A 250 kHz sine wave with a DC component is sampled at a mean sampling frequency 15.625 MHz. At a first step, a pipelined ADC has been chosen to achieve tests and measurements. However, it has been noticed that such architecture of ADC uses a timing block whose role is to eliminate the clock jitter and then change the PDS or PSS output. The most suitable ADC architecture to be used in the case of non-uniform sampling clock is the full flash ADCs [15]. In this paper, tests and measurements are run thanks to an 8-bit full-flash ADC from Maxim,

the MAX100. This ADC operates at a maximum sampling frequency equal to 250 MHz [16].

The spectrum analysis of the acquired samples is presented in Fig. 7. This is a case of pseudorandom delay, with a periodicity equal to  $q - 1$ . The spectrum shows spurious replicas of the sampled signal which is composed of sine-wave signal and a DC signal. The test results confirm the simulation results with replicas at around 20 dB lower than the tested signal.

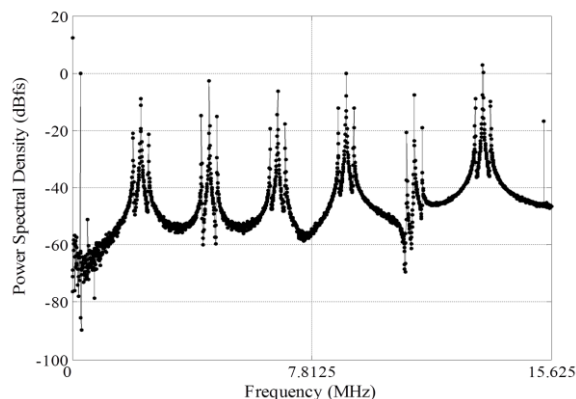


Fig. 7. Test setup results of time-quantized pseudorandom sampled signal.

## V. CONCLUSIONS

In this paper, the authors review the TI-ADC principle and theory in case of both ideal sampling and sampling with mismatches. They propose an equivalent scheme of the TI-ADC and identification by time-quantized pseudorandom sampling technique. This paper offers therefore to the TI-ADC and TQ-PRS communities the opportunity to enlarge the correction process after the use of one of these techniques.

## REFERENCES

- [1] V. Giannini et al., *Baseband Analog Circuits for Software Defined Radio: Analog Circuits and Signal Processing*, New York: Springer-Verlag, 2008
- [2] W. Black and D. Hodges, "Time interleaved converter arrays," *IEEE J. of Solid State Cir.*, vol. 15, no. 6, pp. 1022-1029, Dec. 1980.
- [3] P. Bénabès et al. "Frequency-band-decomposition converters using continuous-time  $\Sigma\Delta$  A/D modulators," *IEEE North-East Workshop on Cir. and Sys. and TAISA Conference*, Jun. 2009.
- [4] A. Eshraghi and T. Fiez, "A comparison of three parallel  $\Delta\Sigma$  A/D converters," *IEEE International Symp. of Cir. and Sys.*, May 1996.
- [5] P. Bénabès et al. "Extended frequency-band-decomposition sigma-delta A/D converter," *Analog Integrated Cir. Proc.*, Jan. 2009.
- [6] D. Camarero et al., "Mixed-signal clock-skew calibration technique for Time-Interleaved ADCs,"

- IEEE Trans. on Cir. and Sys. I: Regular papers, vol. 55, no. 11, pp. 3676-3687, Dec. 2008.
- [7] J.E. Eklund and F. Gustafsson, "Digital offset compensation of timeinterleaved ADC using random chopper sampling," IEEE Inter. Symp. on Cir. and Sys. (ISCAS), May 2000.
- [8] Y.C. Jenq, "Digital Spectra of Nonuniformly Sampled Signals : Fundamentals and High-Speed Waveform Digitizers," IEEE Trans. on Instr. and Measur., vol. 37, no. 2, pp. 245-251, Jun. 1988.
- [9] N. Kurosawa, et al. "Explicit Analysis of Channel Mismatch Effects in Time-Interleaved ADC Systems" IEEE Trans. On Cir. and Sys. —II: fundamental theory and applications, vol 48, no 3, pp 261-271, Mar. 2001.
- [10] M. Ben-Romdhane et al., "Test setup and spurious replicas identification in time-quantized pseudorandom sampling-based ADC in SDR multistandard receiver,". IEEE Int. Conf. on Elect., Cir. and Sys. Dec. 2011.
- [11] A. Maalej, et al., "How Can Time Quantized Random Sampling Reduce Aliases?" submitted to IEEE Trans. On Signal Processing.
- [12] A. Maalej et al., "Towards time-quantized pseudorandom sampling for green communication," IEEE Trans. On Cir. and Sys. II : Brief papers, Vol 61, no 6, pp 443-447, June 2014.
- [13] C. Rebai et al., "Pseudorandom signal sampler for relaxed design of multistandard radio receiver," Microelectronics Journal, Elsevier, vol. 40, pp. 991–999, Jun. 2009.
- [14] A. Maalej et al., "Data Acquisition Test Platform for Non Uniformly Controlled ADC," IEEE Int. Conf. on Design & Technology of Integrated Sys. in Nanoscale Era, Mar. 2010.
- [15] A. Maalej, et al. "Data Acquisition Test Platform for Non Uniformly Controlled ADC" Int. Conf. On Design & Technology of Integrated System in Nanoscale Era, DTIS March, 2010..
- [16] MAX100, 250 MSPS, 8-bit ADC with Track/Hold, MAXIM, Jul. 1994.